Impaired Processing of Human Pro-Islet Amyloid Polypeptide Is Not a Causative Factor for Fibril Formation or Membrane Damage in Vitro[†]

Lucie Khemtémourian,*,‡ Gemma Lahoz Casarramona,§ Dennis P. L. Suylen,‖ Tilman M. Hackeng,‖
Johannes D. Meeldijk,⊥ Ben de Kruijff,‡ Jo W. M. Höppener,§ and J. Antoinette Killian‡

‡*Department of Chemical Biology and Organic Chemistry, Institute of Biomembranes, Utrecht University, Padualaan 8,
3584 CH Utrecht, The Netherlands,* §*Department of Metabolic and Endocrine Diseases, Division of Biomedical Genetics, University
Medical Center Utrecht, P.O. Box 85090, 3508 AB Utrecht, The Netherlands,* ‖*Department of Biochemistry, Cardiovascular Research
Institute Maastricht, Maastricht University, Universiteitssingel 50, 6200 MD Maastricht, The Netherlands, and* ⊥*Department of
Molecular Cell Biology, Electron Microscopy Utrecht, Utrecht University, Padualaan 8, 3584 CH Utrecht, The Netherlands*

ABSTRACT: Human islet amyloid polypeptide (hIAPP) forms amyloid fibrils in pancreatic islets of patients with type 2 diabetes mellitus (DM2). hIAPP is synthesized by islet β-cells initially as a preprohormone, processing of which occurs in several steps. It has been suggested that in DM2 this processing is defective and that aggregation of the processing intermediates prohIAPP and prohIAPP$_{1-48}$ may represent the initial step in formation of islet amyloid. Here we investigate this possibility by analyzing the aggregation, the structure, and the membrane interaction of mature hIAPP and its precursors, prohIAPP and prohIAPP$_{1-48}$, in vitro. Our data reveal that both precursors form amyloid fibrils in solution but not in the presence of membranes. This inhibition is in contrast to the catalyzing effect of membranes on fibril formation of mature hIAPP. Importantly, in the presence of membranes, both precursors are able to inhibit fibrillogenesis of mature hIAPP. These differences in behavior between mature hIAPP and its precursors are most likely related to differences in their mode of membrane insertion. Both precursors insert efficiently and adopt an α-helical structure even with a high lipid/peptide ratio, while mature hIAPP rapidly adopts a β-sheet conformation. Furthermore, while mature hIAPP affects the barrier properties of lipid vesicles, neither of the precursors is able to induce membrane leakage. Our study suggests that the hIAPP precursors prohIAPP and prohIAPP$_{1-48}$ do not serve as amyloid initiators but rather prevent aggregation and membrane damage of mature hIAPP in early stages of its biosynthesis and intracellular transport.

Amyloid formation has been implicated in a wide range of human diseases, including Alzheimer's disease, Parkinson's disease, and type 2 diabetes mellitus (DM2). DM2 is characterized histopathologically by the presence of fibrillar amyloid deposits in the pancreatic islets of Langerhans (islet amyloid). Amyloid cytotoxicity, most likely related to membrane damage, is thought to be an early mechanism involved in the death of insulin-producing islet β-cells in DM2 (1). The main component of islet amyloid, and the actual fibril-forming molecule, is a 37-amino acid peptide called human islet amyloid polypeptide (hIAPP)[1] or amylin, which is produced and secreted together with insulin by the pancreatic islet β-cells. The normal physiological role of soluble hIAPP is not entirely clear, but it is believed to play a role as a hormone in gastric emptying, suppression of food intake, and glucose homeostasis (2−4).

The mechanism of islet amyloid formation is not well understood. One potential cause has been proposed to be alterations in the processing of the hIAPP precursor molecule, prohIAPP, by the islet β-cells (5−7). Insulin and hIAPP are initially synthesized by β-cells as preprohormones, with a N-terminal signal sequence which is cleaved off upon translocation across the endoplasmic reticulum, resulting in the prohormone precursors, proinsulin and prohIAPP, respectively (8). Further processing of these prohormones is a complex process. For prohIAPP [67 amino acids in humans (Figure 1)], it involves cleavage at the C-terminal side in either the trans-Golgi network or in secretory granules, resulting in a processing intermediate of amino acid residues 1−48, prohIAPP$_{1-48}$. This is followed by N-terminal cleavage in the secretory granules resulting in the mature hIAPP (amino acid residues 12−48). Cleavage is initiated at two conserved dibasic sites and involves the prohormone convertases PC3 (also known as PC1) and PC2 (5, 6, 9, 10), which are the same enzymes that process proinsulin to mature insulin. In DM2, processing of proinsulin by β-cells is defective, resulting in an elevated level of release of proinsulin relative to insulin (11, 12). Since proinsulin and prohIAPP are processed in parallel, it is likely that prohIAPP processing may also be defective in DM2, leading to the over-production of unprocessed or partially processed forms of prohIAPP (6, 7). Until now, the precursors have been mostly ignored in studies on the mechanism of amyloid formation by hIAPP because it is believed that their N- and C-terminal

---

*To whom correspondence should be addressed: Department of Chemical Biology and Organic Chemistry, Utrecht University, Padualaan 8, 3584 CH Utrecht, The Netherlands. Telephone: +31 30 2533345. Fax: +31 30 2533969. E-mail: l.p.khemtemourian@uu.nl.

[1]Abbreviations: IAPP, islet amyloid polypeptide; hIAPP, mature human IAPP, corresponding to residues 12−48 of prohIAPP; prohIAPP, pro-islet amyloid polypeptide corresponding to residues 1−67; prohIAPP$_{1-48}$, partially processed pro-islet amyloid polypeptide corresponding to residues 1−48 of prohIAPP; DOPC, 1,2-dioleoyl-*sn*-glycero-3-phosphocholine; DOPS, 1,2-dioleoyl-*sn*-glycero-3-phospho-L-serine; LUVs, large unilamellar vesicles; ThT, thioflavin T.

Published on Web 10/09/2009

peptides	Sequences
ProhIAPP	**TPIESHQVEKR**KCNTATCATQRLANFLVHSSNNFGAILSSTNVGSNTY**GKRNAVEVLKREPLNYLPL**
ProhIAPP$_{1-48}$	**TPIESHQVEKR**KCNTATCATQRLANFLVHSSNNFGAILSSTNVGSNTY
Mature hIAPP	KCNTATCATQRLANFLVHSSNNFGAILSSTNVGSNTY

FIGURE 1: Amino acid sequences of prohIAPP, prohIAPP$_{1-48}$, and mature hIAPP peptides with the N- and C-terminal regions in bold. All three peptides have an intramolecular disulfide bridge. ProhIAPP$_{1-48}$ and mature hIAPP have an amidated C-terminus. The conserved dibasic sites, which are the targets for the prohormone convertases PC1/3 and PC2, are underlined.

extensions do not contribute to the core structure of amyloid fibrils (*13*). However, recent investigations have demonstrated that the precursors do form amyloid aggregates in solution and may be important in early intracellular amyloid formation (*6, 14, 15*). For example, several studies demonstrated that proIAPP interacts with heparan sulfate proteoglycans of the basement membrane that may act as a seed for amyloid formation (*16, 17*). On the other hand, studies of mature hIAPP have shown that membranes can play an active role in amyloid formation. For example, it was shown that the presence of phospholipid membranes can promote hIAPP aggregation, in particular when these membranes contain negatively charged lipids (*18*). In addition, studies of model membranes showed that mature hIAPP inserts into the membrane and causes membrane damage that may lead to cell death in vivo (*17, 19−22*). It is likely that membranes also can influence the aggregation behavior of the precursors prohIAPP$_{1-48}$ and pro-hIAPP, and/or vice versa, that these precursors affect membrane properties. However, despite this potential biological importance, to the best of our knowledge only one study has been published so far on the interaction between membranes and the precursor ProhIAPP, which was obtained via a bacterial expression system (*23*). The results in this paper showed that unlike mature hIAPP, prohIAPP does not form fibrils in the presence of model membranes of phosphatidylcholine and phosphatidylglycerol but an oligomeric-like structure and that proIAPP inhibits fibril formation of mature hIAPP (*23*).

Here, we report a full biophysical study of the behavior of synthetic prohIAPP and prohIAPP$_{1-48}$ in comparison with that of mature hIAPP in the absence and presence of membranes composed of either a 7:3 mixture of phosphatidylcholine (DOPC) and phosphatidylserine (DOPS) in or DOPC only. In particular, we investigate the ability of the precursors to form fibrils, their effect on fibril formation of mature hIAPP, their influence on membrane barrier properties, their insertion into membranes, and their secondary structures. We find that incomplete processing has large consequences for the properties of the peptides as well as for their interaction with membranes and that these consequences point toward less cytotoxic activity of the precursors as compared to mature hIAPP.

EXPERIMENTAL PROCEDURES

Materials. hIAPP was obtained from Bachem AG (lot 0564591). 1,2-Dioleoyl-*sn*-glycero-3-phosphocholine (DOPC) and 1,2-dioleoyl-*sn*-glycero-3-phospho-L-serine (DOPS) were obtained from Avanti Polar Lipids. Thioflavin T was obtained from Sigma.

Synthesis and Purification of ProhIAPP and ProhIAPP$_{1-48}$. ProhIAPP and prohIAPP$_{1-48}$ were synthesized using Boc chemistry using thioester-generating resins and native chemical ligation (*34*). The lysine-cysteine sequence (Figure 1) was chosen as the site of ligation. The peptides were purified by reverse phase high-performance liquid chromatography (HPLC) using Vydac C18 columns (10 μm, 1.0−2.5 cm × 25 cm) and a linear gradient of acetonitrile in water (both containing 0.1% TFA) with flow rates of 5−10 mL/min. The obtained reduced peptides were then folded to yield the internal disulfide bond and purified again by reverse phase HPLC. The identity and purity of peptides were obtained by mass spectrometry. Peptide masses were calculated from the experimental mass to charge (*m/z*) ratios from all the observed protonation states of a peptide. Matrix-assisted laser desorption ionization mass spectrometry (MALDI-MS) was performed on an ABI 4800 MALDI TOF/TOF proteomics analyzer (Applied Biosystems) using α-cyano-4-hydroxycin-namic acid (Aldrich, Milwaukee, WI) as a matrix. Theoretical masses of peptides were calculated using MacProMass (Beckman Research Institute, Duarte, CA).

Preparation of Peptide Samples. Peptide stock solutions were prepared as described previously (*26*). Briefly, peptides were dissolved at a concentration of 1 mM in hexafluoro-2-propanol (HFIP) and incubated for at least 1 h. Next, HFIP was evaporated followed by vacuum desiccation for 20 min. For the CD experiments, the resulting peptide film was then solubi-lized by addition of phosphate buffer or a dispersion of LUVs. For the other experiments, the peptide film was then dissolved in DMSO to a final peptide concentration of 1 mM. For the membrane leakage experiments, thioflavin T assay, and the EM experiments, we used the same concentration of DMSO (2.5%) and hence were able to compare for those experiments the shape of the curve and the lag time.

Preparation of LUVs. The LUVs were composed of either a 7:3 mixture of DOPC and DOPS or DOPC only. Stock solutions of DOPC and DOPS in chloroform at concentrations of 20−30 mM were mixed in a glass tube. The solvent was evaporated with dry nitrogen gas, yielding a lipid film that was subsequently kept in a vacuum desiccator for 20 min. Lipid films were hydrated in 10 mM Tris-HCl and 100 mM NaCl (pH 7.4) during at least 30 min, at a lipid concentration of 10 mM. The lipid suspensions were subjected to 10 freeze−thaw cycles, at temperatures of approximately −80 and 40 °C, and subsequently extruded 10 times through 0.2 μm pore size filters (Anotop 10, Whatman, Maidstone, U.K.). The phospholipid content of lipid stock solutions and vesicle preparations was determined as inorganic phosphate according to Rouser (*35*). Calcein-contain-ing LUVs were made using the same protocol, except for the following adaptations. The buffer for hydration of the lipid film was replaced with a buffer containing 70 mM calcein and 10 mM Tris-HCl (pH 7.4). Free calcein was separated from the calcein-filled LUVs using size-exclusion column chromatography

(Sephadex G-50 fine) and elution with 10 mM Tris-HCl and 100 mM NaCl (pH 7.4).

Electron Microscopy. Peptides and LUVs were incubated under the same conditions as in the thioflavin T assay. Aliquots (20 μL) of this mixture were adsorbed onto glow-discharged carbon-coated 300-mesh copper grids for 2 min. Grids were then blotted and dried. Grids were negatively stained for 45 s on 2% uranyl acetate, blotted, and dried. Grids were examined using a Technai 12 electron microscope operating at 120 kV.

Thioflavin T Assay. The kinetics of fibril formation were measured using the fluorescence intensity increase upon binding of the fluorescent dye thioflavin T (ThT) to fibrils. A plate reader (Spectrafluor, Tecan, Salzburg, Austria) and standard 96-well flat-bottom black microtiter plates in combination with a 430 nm excitation filter and a 535 nm emission filter were used as described previously (*26*). The ThT assay in the presence of membranes was started via addition of 5 μL of a 0.2 mM peptide stock solution in DMSO to 195 μL of a mixture of 10 μM ThT, LUVs (43 μM lipids), 10 mM Tris-HCl, and 100 mM NaCl (pH 7.4). The ThT assay in solution was performed using the same method but without the addition of the LUVs. The microtiter plate was shaken for 9 s, only directly after addition of all components but not during the measurement.

Membrane Permeability Experiments. A plate reader (Spectrafluor, Tecan) was used to perform leakage experiments in standard 96-well transparent microtiter plates. The leakage assay was started via addition of 5 μL of a 0.2 mM hIAPP stock solution in DMSO to 195 μL of a mixture of calcein-containing LUVs (43 μM lipids) with 10 mM Tris-HCl and 100 mM NaCl (pH 7.4). The DMSO concentration of all samples was matched to 2.5% (v/v). Directly after addition of all components, the microtiter plate was shaken for 9 s using the shaking function of the plate reader. The plate was not shaken during the measurement. Fluorescence was measured from the top, every 5 min, using a 485 nm excitation filter and a 535 nm emission filter. The temperature during the measurement was 28 $\pm$ 3 °C. The maximum leakage at the end of each measurement was determined via addition of 1 μL of 10% Triton X-100 to a final concentration of 0.05% (v/v). The release of fluorescent dye was calculated according to eq 1:

$$L(t) = (F_t - F_0)/(F_{100} - F_0) \qquad (1)$$

where $L(t)$ is the fraction of dye released (normalized membrane leakage), F_t is the measured fluorescence intensity, and F_0 and F_{100} are the fluorescence intensities at time zero and after addition of Triton X-100, respectively.

Monolayer Experiments. Peptide-induced changes in the surface pressure of a monomolecular layer of phospholipids at a constant surface area were measured with the Wilhelmy plate method (*36*), as reported previously (*17*). A Teflon trough was filled with 6.0 mL of 10 mM Tris-HCl and 100 mM NaCl (pH 7.4). The subphase was continuously stirred during the measurements. Lipid monolayers were spread from a 1 mM stock solution in chloroform at the air−buffer interface to give initial surface pressures between 20 and 43 mN/m, before 10 μL of a 600 μM freshly prepared stock solution of the peptide in DMSO was injected into the subphase, resulting in a final peptide concentration of 1 μM. DMSO alone, at the concentrations used here, did not affect the surface pressure of the monolayer.

CD Spectroscopy. CD spectra were recorded on a Jasco 810 spectropolarimeter (Jasco Inc., Easton, MD) over the wavelength range of 190−270 nm. Measurements were taken in cells with a path length of 0.1 mm at room temperature in 10 mM phosphate buffer (pH 7.4) and in DOPC/DOPS (7:3) LUVs. Measurements were taken every 0.2 nm at a scan rate of 20 nm/min. Each spectrum reported is the average of five scans after subtraction of the baseline spectrum of the buffer and vesicles without peptide. Peptide concentrations were 25 and 50 μM in buffer and in the presence of lipids (1:9 peptide:lipid ratio).

RESULTS AND DISCUSSION

Membranes Inhibit Fibril Formation of ProhIAPP and ProhIAPP$_{1-48}$. The amino acid sequences of the precursors prohIAPP and prohIAPP$_{1-48}$ and of the mature hIAPP are shown in Figure 1. We first investigated the morphology of the fibrils of prohIAPP and prohIAPP$_{1-48}$ in the absence of membranes by using transmission electron microscopy (TEM). Previous studies on hIAPP precursors showed that they form fibrils in solution, but at a slower rate than mature hIAPP (*14−16*). Consistent with this, we observed the formation of fibrils for mature hIAPP after incubation for 1 day (Figure 2A), while for the same concentration of prohIAPP and prohIAPP$_{1-48}$, approximately 3 days was required to obtain these fibrils (Figure 2B,C). In all cases, the fibrils exhibited the typical morphology of amyloid fibrils with diameters between 10 and 15 nm, consistent with at least two filaments coiled around each other. Next, we followed the kinetics of fibril formation of hIAPP, prohIAPP$_{1-48}$, and prohIAPP in solution by measuring the fluorescence intensity increase upon binding of the amyloid specific dye thioflavin T (ThT), which is a commonly used method for detecting amyloid fibrils (*24*). ThT changes its fluorescence characteristics remarkably upon interaction with amyloids. The kinetics of fibril formation were followed at peptide concentrations of 5 and 10 μM at 25 °C. As shown in Figure 2D, for mature hIAPP an S-shaped curve was obtained, which is a well-known characteristic of amyloid fibril formation (*25*), with a lag time of approximately 4 h for both peptide concentrations. This typical S shape of the fibril formation curve for hIAPP was reproducible for all experiments, but the lag times varied somewhat from 4 to 5 h. With respect to the precursors, the S-shaped curve is only evident for prohIAPP$_{1-48}$, for which we observed a significant increase in ThT fluorescence at 10 μM peptide, with a lag time of approximately 32 h. For 10 μM prohIAPP and for both precursors at lower concentrations, only a very small increase in ThT fluorescence was observed after long incubation times. Control experiments showed that, under the experimental conditions used, the ThT fluorescence for a range between 0.5 and 5% DMSO in the buffer without peptide remains low (data not shown). Together with the TEM data, these results indicate the following order of fibrillogenicity: mature IAPP > prohIAPP$_{1-48}$ > prohIAPP [consistent with previous reports (*14*)].

Next, the same experiments were conducted in the presence of large unilamellar vesicles (LUVs) composed of DOPC and DOPS in a molar ratio of 7:3. After incubation for 1 day with these LUVs, mature hIAPP formed fibrils with a similar morphology as in the absence of membranes, as shown by TEM (Figure 2E). In contrast, for prohIAPP and prohIAPP$_{1-48}$ no fibrils could be detected, even after incubation for 4 days (Figure 2F,G). Figure 1H shows the kinetics of fibril formation as followed by ThT binding. In the presence of membranes, hIAPP fibril formation yields an S-shaped curve with a lag time
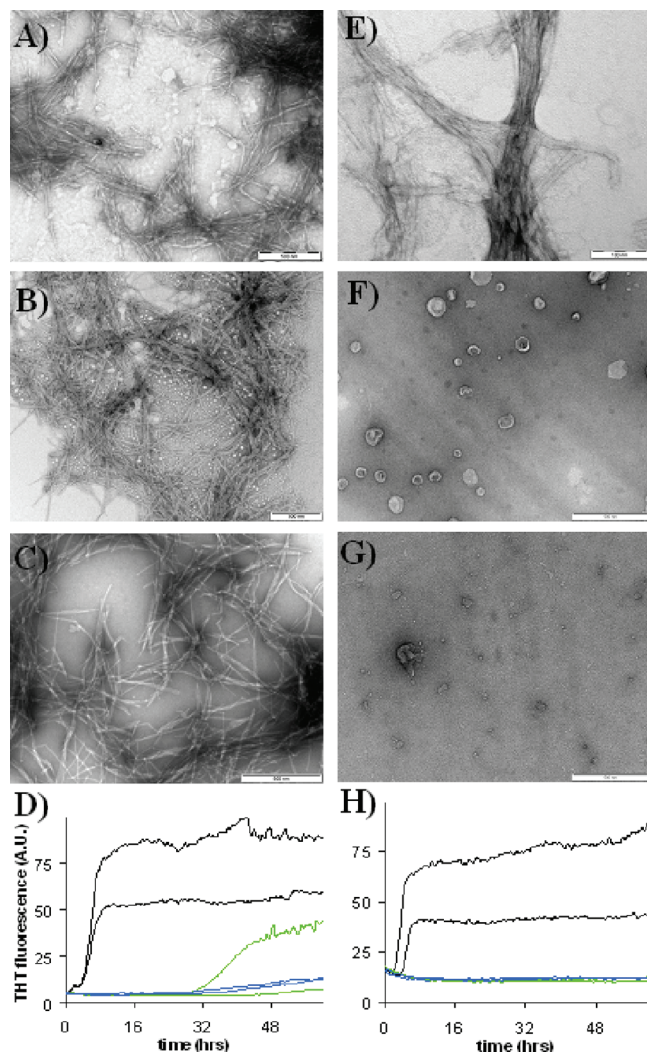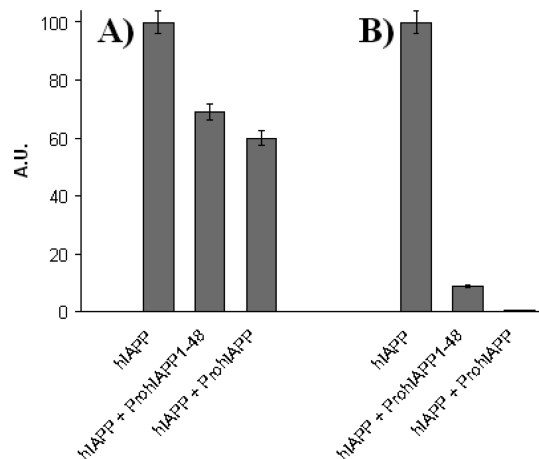
FIGURE 3: Inhibition of mature hIAPP fibril formation by its precursors determined by ThT fluorescence after incubation for 24 h in the presence of DOPC/DOPS membranes. (A) The concentration of mature hIAPP was held constant at $5\,\mu M$, and precursors were added in equimolar amounts to yield 1:1 molar ratio mixtures. (B) The mature hIAPP concentration was held constant at $1\,\mu M$, and the precursors were added at concentrations of $5\,\mu M$ to yield 1:5 molar ratio mixtures. The fluorescence intensities were normalized to the intensity determined for hIAPP without precursors. Data are the average ($\pm$standard deviation) from three independent experiments performed in triplicate.

FIGURE 2: Negatively stained electron microscopy images (A−C and E−G) and ThT fluorescence (D and H) of fibril formation of mature hIAPP and its precursors in 10 mM Tris-HCl and 100 mM NaCl (pH 7.4) in the absence (left) and presence (right) of 7:3 DOPC/DOPS LUVs: (A and E) mature hIAPP after incubation for 1 day (B and F) prohIAPP$_{1-48}$ after incubation for 3 days, (C and G) prohIAPP after incubation for 3 days, and (D and H) hIAPP (black), prohIAPP$_{1-48}$ (green), and prohIAPP (blue) at $10\,\mu M$ (thick) and $5\,\mu M$ (thin).

of approximately 3 h (varying from 2 to 3 h) for both peptide concentrations, indicating that mature hIAPP forms fibrils slightly faster when membranes are present. In contrast, the hIAPP precursors do not seem to form fibrils at all in the presence of membranes, consistent with the TEM data. Also in bilayers composed of zwitterionic lipids (DOPC) only, neither prohIAPP$_{1-48}$ nor prohIAPP was found to form fibrils (data not shown). Control experiments show that, under the experimental conditions used, the ThT fluorescence of DOPC/DOPS and DOPC LUVs without peptide remains low (data not shown). Thus, our results suggest that membranes catalyze fibril formation of mature hIAPP, but that they inhibit fibril formation of its precursors prohIAPP and prohIAPP$_{1-48}$.

hIAPP Precursors Inhibit Fibril Formation of Mature hIAPP in the Presence of Membranes. We next wanted to know whether hIAPP precursors can interfere with mature hIAPP fibrillogenesis in the presence of membranes. Figure 3A shows that when the mature hIAPP concentration was held constant at $5\,\mu M$, addition of the precursors in equimolar amounts resulted in a reduction in the level of fibril formation

to 60−65%, as determined by ThT fluorescence analysis. This was accompanied by an increase in the lag time from 2−3 to 3−5 h (not shown).

The same experiment was conducted with $1\,\mu M$ mature hIAPP, and hence a 5-fold molar excess of precursors. As shown in Figure 3B, under these conditions, mature hIAPP fibrillogenesis was almost completely blocked. These data demonstrate that both hIAPP precursors inhibit fibril formation of mature hIAPP.

ProhIAPP$_{1-48}$ and ProhIAPP Do Not Induce Membrane Leakage. Previously, for mature hIAPP, a correlation was found between fibril formation and peptide-induced membrane damage (*26*). It was postulated that fibril formation of hIAPP at the membrane surface causes hIAPP-induced membrane damage. If these processes of fibril formation and membrane damage are indeed causally related, we would expect that the precursors will not be able to induce membrane leakage, based on our observation that membranes inhibit fibril formation of the precursors. Membrane damage was assayed quantitatively by analyzing the extent of leakage of a fluorescent dye (calcein) from large unilamellar vesicles (LUVs), which is an established membrane leakage assay for studying membrane interactions of amyloidogenic peptides (*27, 28*). Figure 4A shows that in DOPC/DOPS LUVs at $5\,\mu M$ peptide mature hIAPP is able to induce ∼60% of membrane leakage after incubation for 6 h, while prohIAPP$_{1-48}$ and prohIAPP do not affect barrier properties of lipid vesicles (<10% leakage), after incubation for 24 h (Figure 4B,C). For mature hIAPP, the lag time was ∼2 h. The same results were observed with only DOPC membranes (data not shown). After incubation for 24 h, mature hIAPP induces membrane leakage while prohIAPP$_{1-48}$ and prohIAPP do not. Control experiments showed that, under the experimental conditions used, 2.5% DMSO in the presence of DOPC/DOPS or DOPC LUVs does not induce membrane leakage (data not shown). Thus, while mature hIAPP does form fibrils and induces membrane leakage, the precursors do neither. This is consistent with the recent notion, based on simulation studies, that highly
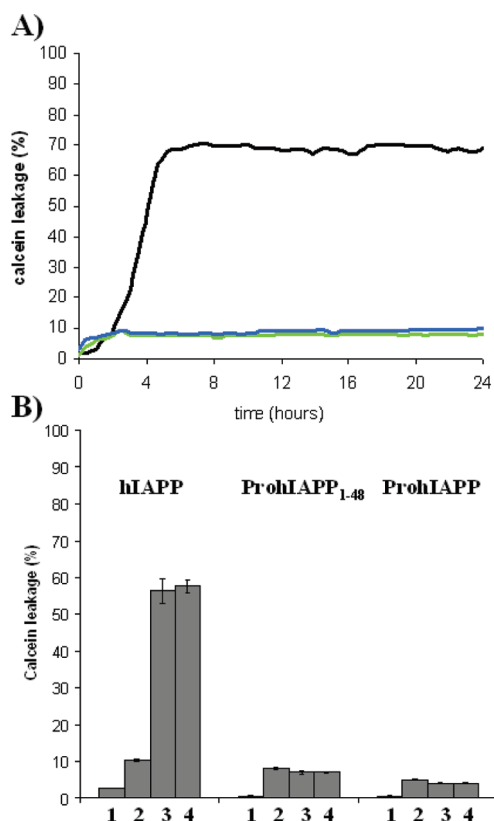
A)

B)

FIGURE 4: (A) Kinetics of membrane permeabilization by 5 μM mature hIAPP (black), prohIAPP$_{1-48}$ (green), and prohIAPP (blue). The peptides were added to the calcein-containing DOPC/DOPS (7:3) LUVs at time zero. The maximum leakage, after complete disruption of all vesicles by Triton, was set to 1. (B) Membrane damage by 5 μM mature hIAPP, prohIAPP$_{1-48}$, and prohIAPP after prolonged incubation with calcein-loaded LUVs. Vesicle leakage was determined after incubation of LUVs for 1 min, 2 h, 6 h, and 24 h with peptides (1−4, respectively). Data are the average (±standard deviation) from three independent experiments performed in triplicate.

fibrillogenic peptides form fibrils more rapidly in the presence of lipid vesicles than in their absence, while the opposite is observed for peptides of low fibrillogenicity, where fibril formation is slower in the presence of lipid vesicles (*29*). It is likely that the observed differences in membrane interaction between mature hIAPP and its precursors are caused by differences in membrane insertion and/or differences in the conformational behavior of the peptides. This was investigated next.

Do ProhIAPP and ProhIAPP$_{1-48}$ Insert Efficiently into a Membrane?. To study the insertion of peptides in lipid membranes, we performed monolayer experiments. Insertion of peptides into a monolayer of phospholipids at the air−/water interface can be monitored as an increase in the surface pressure of the monolayer (*30*). Injection of a solution of hIAPP, prohIAPP, or prohIAPP$_{1-48}$ in the aqueous subphase below a DOPC/DOPS (7:3) monolayer results in a fast increase in the surface pressure, followed by a plateau starting approximately 5 min after the addition of each peptide (Figure 5A). After 25 min, the increase in surface pressure induced by insertion of hIAPP is 9 mN/m, compared to an increase of 13 mN/m for prohIAPP and 16 mN/m for prohIAPP$_{1-48}$. Again, similar results were obtained in a DOPC monolayer (data not shown). These results demonstrate that both precursors have a very strong capacity to insert into lipid monolayers.

Next, we set out to determine the maximal initial surface pressure at which the peptides were still able to insert, i.e., cause a
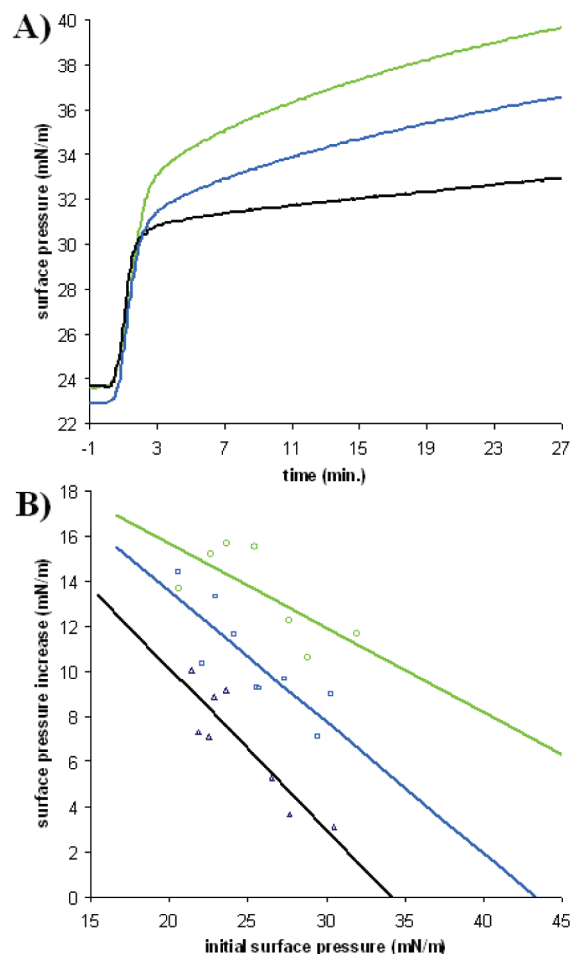
A)

B)

FIGURE 5: (A) Surface pressure profile after injection of a sample of hIAPP (black), a sample of prohIAPP$_{1-48}$ (green), and a sample of prohIAPP (blue) in a DOPC/DOPS monolayer (7:3). The peptides were injected into the stirred subphase at time zero. The final peptide concentration was 1 μM. (B) Surface pressure increase induced by the interaction of freshly dissolved hIAPP ($\triangle$), prohIAPP$_{1-48}$ ($\square$), and prohIAPP ($\bigcirc$) with DOPC/DOPS (7:3) monolayers as a function of the initial surface pressure. The straight lines were obtained by linear regression.

further increase in surface pressure, by analyzing the surface pressure increase as a function of initial surface pressure. The data from Figure 5B indicate that this "limiting surface pressure" is high for all peptides and appears to be higher for prohIAPP$_{1-48}$ than for prohIAPP and mature hIAPP. In both cases, for prohIAPP and prohIAPP$_{1-48}$, the (extrapolated) limiting surface pressure is significantly higher than the surface pressures that correspond to the packing density in lipids in biological membranes, being between 31 and 35 mN/m (*31*), indicating also that in vivo mature hIAPP and its precursors can insert efficiently into membranes.

Membranes Promote an α-*Helical Conformation for ProhIAPP and ProhIAPP$_{1-48}$.* Next, we used CD spectroscopy to investigate the structure of hIAPP and its precursors in the absence and presence of membranes. The CD spectrum of mature hIAPP (Figure 6A, black) freshly dissolved in 10 mM phosphate buffer at 25 μM displays a peak with negative ellipticity at 198 nm that is characteristic of a random coil conformation, in agreement with previous studies (*28*, *32*). However, at a higher concentration (50 μM), the CD spectrum displays a peak at 220 nm that indicates a β-sheet conformation. On the other hand, at the same concentrations, the spectra of
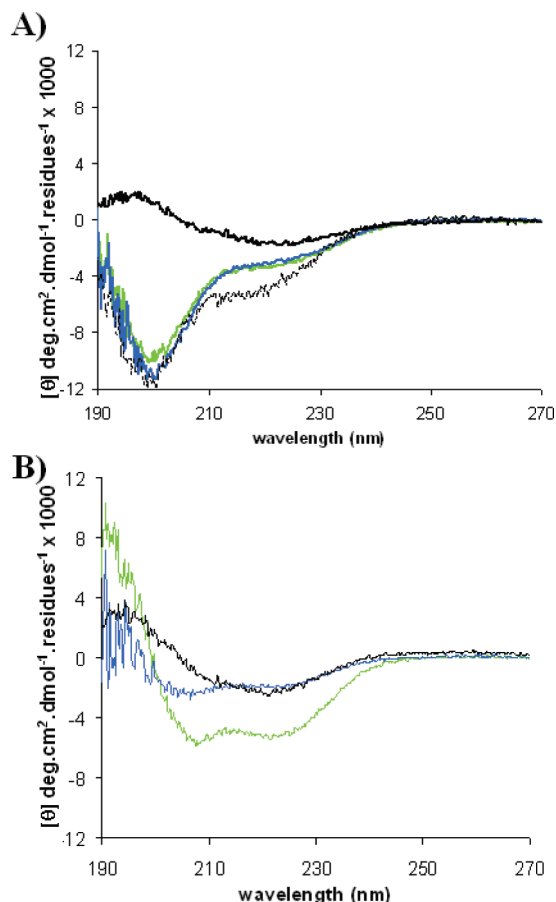
A)

B)

FIGURE 6: CD spectra of prohIAPP$_{1-48}$ (green), prohIAPP (blue), and mature hIAPP at 50 μM (black solid line) and 25 μM (black dotted line) in 10 mM phosphate buffer (pH 7.4) in the absence (A) and presence (B) of 7:3 DOPC/DOPS LUVs (1:9 lipid:peptide ratio).
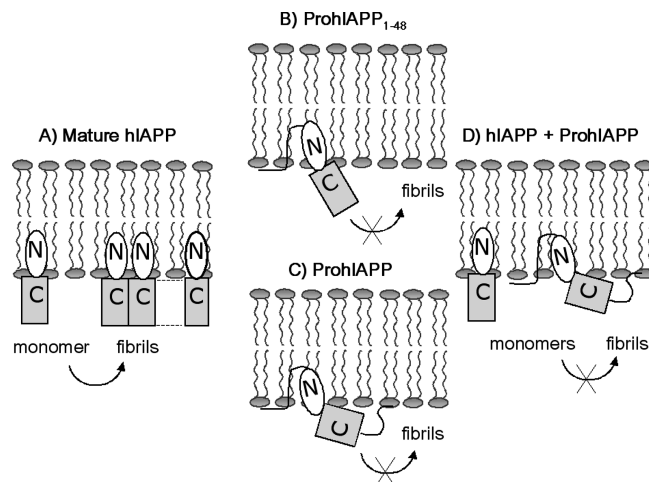

FIGURE 7: Simplified schematic representation of the proposed hypothesis that hIAPP precursors serve to protect the mature hIAPP against fibrillogenesis. Mature hIAPP inserts into the membrane and is able to form fibrils (A). The precursors (prohIAPP$_{1-48}$ B and prohIAPP C) insert into the membrane, where the N- and C-terminal extensions cause inhibition of fibril formation. The precursors inhibit fibril formation of mature hIAPP (D). For details, see the text.

prohIAPP and prohIAPP$_{1-48}$ (Figure 6A, blue and green, respectively) always display a peak with negative ellipticity at 198 nm and indicate a predominantly unordered backbone structure. Thus, in solution and at high concentrations, the precursors do not adopt the same conformation as the mature hIAPP, in agreement with previous studies (*15, 16, 23*).

The same experiments were conducted in the presence of 7:3 DOPC/DOPS LUVs. In agreement with previous studies (*32*), the CD spectrum of mature hIAPP at 25 μM exhibited negative ellipticity at 208 and 222 nm, characteristic of an α-helical backbone structure (Figure 6B, black dotted line). However, at a higher concentration (50 μM), the CD spectrum displays a single peak with negative ellipticity at 220 nm, which indicates a β-sheet conformation (Figure 6B, black). In contrast, spectra of prohIAPP and prohIAPP$_{1-48}$ at 50 μM (Figure 6B, green and blue, respectively) recorded immediately after the addition of LUVs display negative ellipticity at 208 and 222 nm, characteristic of an α-helical backbone structure. For prohIAPP$_{1-48}$, the minima are more prominent compared to those of prohIAPP, suggesting that prohIAPP$_{1-48}$ has a greater α-helix content than prohIAPP. The observation that the precursors adopt a stable α-helical structure even with a high concentration and a high lipid: peptide ratio (1:9) suggests that the N- and C-terminal flanking residues stabilize an α-helical conformation of the mature part of the peptide.

Model for the Differences in Membrane Interaction between Mature hIAPP and Its Precursors. A model based on our data is depicted in Figure 7. The N-terminal part of

mature hIAPP inserts into the membrane, which catalyzes the fibrillogenesis, possibly by concentrating the peptide at the bilayer surface and positioning the most amyloidogenic regions (postulated to be located near residues 20−29 in mature hIAPP) in such a way that aggregation is promoted, as described previously (*17, 28*) (Figure 7A). Like hIAPP, the precursors also insert into the membrane, but in this case, the interaction results in inhibition of fibril formation (Figure 7B,C), most likely because of steric hindrance. For prohIAPP$_{1-48}$ (Figure 7B), this inhibition could result from (partial) insertion of its N-terminal part into the membrane, perhaps combined with a change in the orientation and/or conformation of the mature part with respect to the lipid bilayer interface. In the case of prohIAPP (Figure 7C), both the N- and C-terminal part may interact with the lipids and thereby more strongly inhibit aggregation. In addition, for both precursors, the flanking sequences may stabilize an α-helical structure of the mature part and thereby inhibit β-sheet formation, which is the required conformation for fibrillogenesis. In the presence of mature hIAPP, both precursors can insert into the membrane (Figure 7D), where they can decrease the rate and extent of hIAPP fibril formation by steric hindrance. Hence, the precursors might serve to protect the mature hIAPP against fibrillogenesis.

SUMMARIZING CONCLUSIONS

Two important conclusions can be drawn from the results of this study. First, the results clearly show that the precursors prohIAPP$_{1-48}$ and prohIAPP are less fibrillogenic than mature hIAPP, also in the presence of membranes. This is consistent with previous studies of the precursors in solution and also with a recent study by Winter and co-workers on the interaction of prohIAPP with model membranes (*23*). Given the dependence of the behavior of amyloid-forming molecules on specific experimental conditions and the relative complexity in terms of possible variables in the membrane-containing systems, this is strong support for the general validity of this conclusion. The second important conclusion from this study is that membranes, while catalyzing fibril formation of mature IAPP, in fact inhibit fibril

formation of these precursors. It appears reasonable to suggest that the precursors of mature hIAPP could serve to protect the mature peptide against fibrillogenesis in the β-cells, where they are present at relatively high concentrations, rather than being a trigger of amyloid fibril formation. Hence, one of the functions of the N- and C-terminal parts of ProhIAPP may be to prevent aggregation and fibrillogenesis in early stages of hIAPP biosynthesis and transport through the secretory pathways, as suggested by other groups (*14, 15, 23*). However, we note that this does not imply that misprocessing of prohIAPP in vivo should have a protecting effect on fibril formation. For example, it is possible that any such putative protective effect might be counteracted by a simultaneous misprocessing of insulin. This is an intriguing possibility in light of the recent suggestion that impaired processing of prohIAPP is a causative factor in generating intracellular hIAPP deposits found in DM2 models and in humans (*5, 6, 33*). Clearly, more studies on interactions between the precursors of hIAPP and of insulin in the presence of membranes will be required to shed light on their possible consequences for hIAPP fibril formation.

ACKNOWLEDGMENT

REFERENCES

1. Höppener, J. W., Ahren, B., and Lips, C. J. (2000) Islet amyloid and type 2 diabetes mellitus. *N. Engl. J. Med. 343*, 411–419.
2. Akesson, B., Panagiotidis, G., Westermark, P., and Lundquist, I. (2003) Islet amyloid polypeptide inhibits glucagon release and exerts a dual action on insulin release from isolated islets. *Regul. Pept. 111*, 55–60.
3. Reda, T. K., Geliebter, A., and Pi-Sunyer, F. X. (2002) Amylin, food intake, and obesity. *Obes. Res. 10*, 1087–1091.
4. Rushing, P. A., Hagan, M. M., Seeley, R. J., Lutz, T. A., D'Alessio, D. A., Air, E. L., and Woods, S. C. (2001) Inhibition of central amylin signaling increases food intake and body adiposity in rats. *Endocrinology 142*, 5035–5038.
5. Marzban, L., Rhodes, C. J., Steiner, D. F., Haataja, L., Halban, P. A., and Verchere, C. B. (2006) Impaired NH₂-terminal processing of human proislet amyloid polypeptide by the prohormone convertase PC2 leads to amyloid formation and cell death. *Diabetes 55*, 2192–2201.
6. Paulsson, J. F., Andersson, A., Westermark, P., and Westermark, G. T. (2006) Intracellular amyloid-like deposits contain unprocessed pro-islet amyloid polypeptide (proIAPP) in β cells of transgenic mice overexpressing the gene for human IAPP and transplanted human islets. *Diabetologia 49*, 1237–1246.
7. Paulsson, J. F., and Westermark, G. T. (2005) Aberrant processing of human proislet amyloid polypeptide results in increased amyloid formation. *Diabetes 54*, 2117–2125.
8. Kahn, S. E., D'Alessio, D. A., Schwartz, M. W., Fujimoto, W. Y., Ensinck, J. W., Taborsky, G. J.Jr., and Porte, D.Jr. (1990) Evidence of cosecretion of islet amyloid polypeptide and insulin by β-cells. *Diabetes 39*, 634–638.
9. Marcinkiewicz, M., Ramla, D., Seidah, N. G., and Chretien, M. (1994) Developmental expression of the prohormone convertases PC1 and PC2 in mouse pancreatic islets. *Endocrinology 135*, 1651–1660.
10. Furuta, M., Yano, H., Zhou, A., Rouille, Y., Holst, J. J., Carroll, R., Ravazzola, M., Orci, L., Furuta, H., and Steiner, D. F. (1997) Defective prohormone processing and altered pancreatic islet morphology in mice lacking active SPC2. *Proc. Natl. Acad. Sci. U.S.A. 94*, 6646–6651.
11. Kahn, S. E., and Halban, P. A. (1997) Release of incompletely processed proinsulin is the cause of the disproportionate proinsulinemia of NIDDM. *Diabetes 46*, 1725–1732.
12. Ward, W. K., LaCava, E. C., Paquette, T. L., Beard, J. C., Wallum, B. J., and Porte, D.Jr. (1987) Disproportionate elevation of immunoreactive proinsulin in type 2 (non-insulin-dependent) diabetes mellitus and in experimental insulin resistance. *Diabetologia 30*, 698–702.

13. Jaikaran, E. T., Higham, C. E., Serpell, L. C., Zurdo, J., Gross, M., Clark, A., and Fraser, P. E. (2001) Identification of a novel human islet amyloid polypeptide β-sheet domain and factors influencing fibrillogenesis. *J. Mol. Biol. 308*, 515–525.
14. Yonemoto, I. T., Kroon, G. J., Dyson, H. J., Balch, W. E., and Kelly, J. W. (2008) Amylin proprotein processing generates progressively more amyloidogenic peptides that initially sample the helical state. *Biochemistry 47*, 9900–9910.
15. Krampert, M., Bernhagen, J., Schmucker, J., Horn, A., Schmauder, A., Brunner, H., Voelter, W., and Kapurniotu, A. (2000) Amyloidogenicity of recombinant human pro-islet amyloid polypeptide (ProIAPP). *Chem. Biol. 7*, 855–871.
16. Meng, F., Abedini, A., Song, B., and Raleigh, D. P. (2007) Amyloid formation by pro-islet amyloid polypeptide processing intermediates: Examination of the role of protein heparan sulfate interactions and implications for islet amyloid formation in type 2 diabetes. *Biochemistry 46*, 12091–12099.
17. Engel, M. F. M., Yigittop, H., Elgersma, R. C., Rijkers, D. T., Liskamp, R. M., de Kruijff, B., Höppener, J. W., and Killian, J. A. (2006) Islet amyloid polypeptide inserts into phospholipid monolayers as monomer. *J. Mol. Biol. 356*, 783–789.
18. Knight, J. D., and Miranker, A. D. (2004) Phospholipid catalysis of diabetic amyloid assembly. *J. Mol. Biol. 341*, 1175–1187.
19. Demuro, A., Mina, E., Kayed, R., Milton, S. C., Parker, I., and Glabe, C. G. (2005) Calcium dysregulation and membrane disruption as a ubiquitous neurotoxic mechanism of soluble amyloid oligomers. *J. Biol. Chem. 280*, 17294–17300.
20. Kayed, R., Sokolov, Y., Edmonds, B., McIntire, T. M., Milton, S. C., Hall, J. E., and Glabe, C. G. (2004) Permeabilization of lipid bilayers is a common conformation-dependent activity of soluble amyloid oligomers in protein misfolding diseases. *J. Biol. Chem. 279*, 46363–46366.
21. Porat, Y., Kolusheva, S., Jelinek, R., and Gazit, E. (2003) The human islet amyloid polypeptide forms transient membrane-active prefibrillar assemblies. *Biochemistry 42*, 10971–10977.
22. Anguiano, M., Nowak, R. J., and Lansbury, P. T.Jr. (2002) Protofibrillar islet amyloid polypeptide permeabilizes synthetic vesicles by a pore-like mechanism that may be relevant to type II diabetes. *Biochemistry 41*, 11338–11343.
23. Jha, S., Sellin, D., Seidel, R., and Winter, R. (2009) Amyloidogenic Propensities and Conformational Properties of ProIAPP and IAPP in the Presence of Lipid Bilayer Membranes. *J. Mol. Biol. 389*, 907–920.
24. LeVine, H.III (1999) Quantification of β-sheet amyloid fibril structures with thioflavin T. *Methods Enzymol. 309*, 274–284.
25. Padrick, S. B., and Miranker, A. D. (2002) Islet amyloid: Phase partitioning and secondary nucleation are central to the mechanism of fibrillogenesis. *Biochemistry 41*, 4694–7403.
26. Engel, M. F. M., Khemtémourian, L., Kleijer, C. C., Meeldijk, H. J., Jacobs, J., Verkleij, A. J., de Kruijff, B., Killian, J. A., and Höppener, J. W. (2008) Membrane damage by human islet amyloid polypeptide through fibril growth at the membrane. *Proc. Natl. Acad. Sci. U.S.A. 105*, 6033–6038.
27. McLaurin, J., and Chakrabartty, A. (1996) Membrane disruption by Alzheimer β-amyloid peptides mediated through specific binding to either phospholipids or gangliosides. Implications for neurotoxicity. *J. Biol. Chem. 271*, 26482–26489.
28. Knight, J. D., Hebda, J. A., and Miranker, A. D. (2006) Conserved and cooperative assembly of membrane-bound α-helical states of islet amyloid polypeptide. *Biochemistry 45*, 9496–9508.
29. Friedman, R., Pellarin, R., and Caflisch, A. (2009) Amyloid aggregation on lipid bilayers and its impact on membrane permeability. *J. Mol. Biol. 387*, 407–415.
30. Demel, R. A., London, Y., Geurts van Kessel, W. S., Vossenberg, F. G., and van Deenen, L. L. (1973) The specific interaction of myelin basic protein with lipids at the air-water interface. *Biochim. Biophys. Acta 311*, 507–519.
31. Demel, R. A., Geurts van Kessel, W. S., Zwaal, R. F., Roelofsen, B., and van Deenen, L. L. (1975) Relation between various phospholipase actions on human red cell membranes and the interfacial phospholipid pressure in monolayers. *Biochim. Biophys. Acta 406*, 97–107.
32. Jayasinghe, S. A., and Langen, R. (2005) Lipid membranes modulate the structure of islet amyloid polypeptide. *Biochemistry 44*, 12113–12119.
33. de Koning, E. J., Morris, E. R., Hofhuis, F. M., Posthuma, G., Höppener, J. W., Morris, J. F., Capel, P. J., Clark, A., and Verbeek, J. S. (1994) Intra- and extracellular amyloid fibrils are formed in cultured pancreatic islets of transgenic mice expressing human

islet amyloid polypeptide. *Proc. Natl. Acad. Sci. U.S.A. 91*, 8467–8471.

34. Hackeng, T. M., Griffin, J. H., and Dawson, P. E. (1999) Protein synthesis by native chemical ligation: Expanded scope by using straightforward methodology. *Proc. Natl. Acad. Sci. U.S.A. 96*, 10068–10073.

35. Rouser, G., Fleischer, S., and Yamamoto, A. (1970) Two dimensional thin layer chromatographic separation of polar lipids and determination of phospholipids by phosphorus analysis of spots. *Lipids 5*, 494–496.

36. Demel, R. A. (1994) Monomolecular layers in the study of biomembranes. *Subcell. Biochem. 23*, 83–120..